Eur. Phys. J. Special Topics **228**, 2441–2454 (2019)

https://doi.org/10.1140/epjst/e2019-900007-8

THE EUROPEAN PHYSICAL JOURNAL SPECIAL TOPICS

Regular Article

Intralayer synchronization in neuronal multiplex network

Bidesh K. Bera[1], Sarbendu Rakshit[2], and Dibakar Ghosh[2,a]

[1] Department of Mathematics, Indian Institute of Technology Ropar, Rupnagar 140001, Punjab, India
[2] Physics and Applied Mathematics Unit, Indian Statistical Institute, Kolkata 700108, India

Received 22 January 2019 / Received in final form 6 March 2019
Published online 28 October 2019

Abstract. Synchronization phenomenon is one of the most fundamental properties in the field of neurosciences, and it plays a key role in several neuronal processes. In this paper, we report a neural synchrony in a multiplex neuronal network by simultaneously taking electrical and chemical synaptic interactions. Most of the previous studies on the neuronal synchrony have been focused on a mono-layer network by solely considering one type of neuronal communication, either electrical or chemical synaptic coupling. Here we consider the multiplex network where the connection within the layer (intralayer connection) and the layer–layer interaction (interlayer connection) links are associated with the electrical and chemical synapses respectively. The network topology in each layer is represented by the small-world network. We mainly explore intralayer synchronization in the multiplex network under the simultaneous effect of both synaptic interactions. Intralayer synchronization is a distinctive process that refered to coherence among the nodes within the layer irrespective of the coherence between the replica nodes. Through the master stability approach, we derive the necessary condition for the intralayer synchronization state and then we numerically confirm our analytical findings.

1 Introduction

Complex network theory [1–4] is one of the most cultivated subject due to its immense necessity and applicability in several fields of science and technology. This theory helps a lot in modelling the various types of systems, ranging from microscopic level to a large complex system. The main advantage of this theory is that it provides a prolific ground for understanding the several universal properties of the large number of interacting complex dynamical units. In the real-world situation, naturally arising systems are typically connected to each other in various ways depending on their nature of interaction processes. The combined effect of the coupling mechanism and associated underlying interacting topology among the agents plays a vital role in their normal functioning. Some dynamical processes which are often associated with networks and the investigation into emergent unfolding collective phenomena have

[a] e-mail: diba.ghosh@gmail.com

gained considerable attention in the last few decades [5–7]. Among them synchronization phenomenon is one of the most interesting research topic from the nonlinear science perspective [8–13]. A detailed study of this property has been done by considering various types of complex networks such as random network [14], scale-free network [15], small-world network [16] and also different types of regular networks. Yet, there are many synchronization processes where the network does not involve a single network, rather they rely on this property by the collection of various networks. Such scenarios are observed in the power grid networks, ecological network and neuronal systems.

Network architecture is the main backbone of the various complex systems. Recently, several extensions of the complex network have been developed to carefully capture the structural properties of the networks which include hypernetwork [17–19], modular network [20], multilayered network [21–23], etc. Among them multilayer network formation is a rapidly evolving research field in recent times. This network architecture describes various real-world networks [24] in a beautiful way. Such networks consist of diverse layers, which either simultaneously exist or alternate with respect to time [21,22]. For illustration, consider an online social networking system where each individual is connected through Facebook, twitter or Instagram or some combination of these three social systems. If we consider each social system represents a layer then each layer has its own interacting pattern, yet the individuals typically influence each other across layers [25]. A similar type of connectivity pattern is observed in inter-neuronal communication [26]. In the neuronal network, neurons interact through two types of synapses. One is electrical coupling via the gap-junctional channels and another one is chemical synaptic interaction [26]. A study on multilayer network offers to better understand the several interaction processes, ranging from brain network to social communication; in particular, social network [27] where the people from one community are connected to other communities via different types of relations, mobility network [28,29] where each individual is served with various types of transportations. Also air transportation network [30], subway network [31,32], epidemic spreading process [33], neuronal network [34] all have the best representation in the multilayer network formations. Moreover, such architectures uncover some interesting emerging collective phenomena such as percolation [35–37] and diffusion processes [38], epidemic spreading [39–41], evolutionary game dynamics [42], controllability theory [43] and chimera states [44,45]. This phenomenology of multilayer network is quite different from the results on single layer or monolayer network.

Multilayer network mainly consists of two types of interactions, one is intralayer interaction which defines the interaction among the nodes within layer and another is interlayer interaction which refers to the connection between the nodes which are located in different layers. The intralayer interaction types within the layers may differ from the other layer as well as from the interlayer interactions. When the different layers are composed with an equal number of nodes and the interlayer connections between the same nodes are preserved in such a way that a node from one layer is only linked with its replica node in the remaining layers, then such a multilayer structure is called a *multiplex network.* In this network formation various types of synchrony phenomena were investigated such as intra- and inter-layer synchronizations [46–50], explosive synchronization [51], coexistence of synchrony and desynchrony [53–56], and cluster synchronization [57]. In addition solitary states for a multiplex architecture was also observed in reference [52] in the presence of both positive and negative couplings.

Brain functions are mainly dependent on the interneuronal communications between neurons, in which each neuron relies or exchanges the information to other neurons via synaptic communications. Originally, two types of synapses are observed,

one is electrical coupling and the other one is chemical synapse. The first type of interaction takes place between two adjacent nodes by making a gap-junctional channel between them and the latter one happens chemically from pre- to post-synaptic neurons. The simultaneous presence of these two types of synaptic interactions was noticed in most of the nervous systems, and they are performed independently [26]. Such a type of neuronal synaptic communication arrangement is perfectly perceived by designing a multiplex neuronal network. Synchronization phenomenon is one of the most essential properties in the field of neurosciences [58], since the different types of the abnormal patterns of synchrony [59–61] in the brain are closely related to several brain disorder [62] diseases, which include, Alzheimer's, epilepsy, schizophrenia and Parkinson's diseases. The different types of neuronal synchronization patterns were observed experimentally [63–65] by performing the experiment on the series of neuronal systems, such as human thalamocortical area, and human cardiorespiratory system [66], mammalian visual cortex, ganglion of the spiny lobster and stomatogastric, etc. Most of the previous results on the neuronal synchrony were concentrated on taking either electrical or chemical synaptic interactions as the underlying interacting topology is a single network formation or monolayer architecture. But from the neurobiological perspective, the study of neuronal synchrony in the multiplex structure has immense importance and deserves special attention.

Inspired by the above facts, we investigate the neuronal synchrony in the multiplex neuronal network. Each layer of the network is represented by a small-world network architecture. The emergence of small-world connectivity in the brain network is discussed by Bassett et al. [67,68] in their pioneering review article. In our study, the local dynamics of the each node of the neuronal network are cast with the Hindmarsh–Rose neuron which is a well established neuronal oscillator and is known for different types of bursting and spiking behaviors. Motivated from the neuroscience point of view, in our work, we consider the intralayer interaction type is electrical communication, whereas the interlayer link is realized through chemical synaptic interaction. Here we explore the complete intralayer synchronization property of the multiplex neuronal network under the combined effect of these two synaptic interactions. Through the linear stability approach, we analytically derive necessary and sufficient conditions for the existence of the intralayer synchronization state and we characterize the state by master stability function framework. The analytical findings are testified by the numerical results.

2 Mathematical model of neuronal multiplex network

For the multiplex neuronal network, we consider two layers where each layer is composed of N Hindmarsh–Rose (HR) neurons connected through electrical synapses and the layers are connected among themselves through chemical synapses. Since our main goal was to study complete intralayer synchronization, we keep each HR neuron identical. The mathematical description of the entire neuronal network model can be described as

$$\text{Layer} - 1:$$

$$\dot{x}_{1i} = (a - x_{1i})x_{1i}^2 - y_{1i} - z_{1i} + \epsilon \sum_{j=1}^{N} \mathscr{A}_{ij}^{[1]}(x_{1j} - x_{1i}) + g_c(v_s - x_{1i})\,\Gamma(x_{2i}),$$

$$\dot{y}_{1i} = (a + \alpha)x_{1i}^2 - y_{1i},$$

$$\dot{z}_{1i} = \mu(bx_{1i} + c - z_{1i}),$$

$$\text{Layer} - 2: \tag{1}$$

$$\dot{x}_{2i} = (a - x_{2i})x_{2i}^2 - y_{2i} - z_{2i} + \epsilon \sum_{j=1}^{N} \mathscr{A}_{ij}^{[2]}(x_{2j} - x_{2i}) + g_c(v_s - x_{2i})\ \Gamma(x_{1i}),$$

$$\dot{y}_{2i} = (a + \alpha)x_{2i}^2 - y_{2i},$$

$$\dot{z}_{2i} = \mu(bx_{2i} + c - z_{2i}),$$

where $i = 1, 2, \ldots, N$ is the neuron index and N is the total number of neurons in each layer. Here (x_{li}, y_{li}, z_{li}) denotes the state variable of the ith-node in layer-l, in which x_{li} denotes the membrane potential of the ith-neuron, y_{li} corresponds to the transport of ions across the membrane through fast currents associated with Na^+ or K^+, z_{li} be the slow Ca^{2+} current and μ modulate the slow dynamics of the system. Let the control parameter ϵ be the intralayer interaction strength corresponding to electrical synapses, which determine how much information will be distributed among the neurons. The overall strength of interaction between the two layers is tuned by the chemical synaptic strength g_c. We fixed the parameter $a = 2.8, b = 9.0, c = 5.0, \alpha = 2.8$, and $\mu = 0.005$ for which the membrane potential of an isolated neuron displays multi-time scale chaotic spiking-bursting disposition. The nonlinear sigmoidal input–output function $\Gamma(\mathbf{x}) = \frac{1}{1+\exp[-\lambda(\mathbf{x}-\Theta_s)]}$ delineates the mechanism of the activation and deactivation for the chemical synapses. Here v_s is the synaptic reversal potential. For $v_s > x_{li}(t)$ the synaptic current has a depolarizing effect making the synapse excitatory, and the synaptic current exhibits hyper-polarizing effect for $v_s < x_{li}(t)$ which makes the synapse inhibitory. For our system parameters, $|x_{li}(t)|$ is always less than 2, thus $(x_{li}(t) - v_s)$ becomes negative for $v_s = 2.0$, hence the chemical synapse is excitatory forever. So spiking of the pre-synaptic neuron induces the post-synaptic neuron to spike. Parameter Θ_s controls the synaptic firing threshold and the slope of the sigmoidal function is determined by λ, hereafter $\Theta_s = -0.25$ and $\lambda = 10$.

Here one neuron in a layer is connected to its replica on the other layer by the chemical ion transportation through chemical synapses and the intralayer couplings are considered through bidirectional electrical gap junctional couplings. The connectivity of the intralayer electrical synapses are deliberated as bidirectional small-world networks, described by the adjacency matrix $\mathscr{A}_{ij}^{[l]}$ (where in layer-l, $\mathscr{A}_{ij}^{[l]} = 1$ if ith-node is connected to jth-node and 0 otherwise), for $l = 1, 2$. The corresponding zero-row sum Laplacian matrices are given by $\mathscr{L}_{ij}^{[l]} = -\mathscr{A}_{ij}^{[l]}$ for $i \neq j$, and $\mathscr{L}_{ii}^{[l]} = \sum_{j=1}^{N} \mathscr{A}_{ij}^{[l]}$. Let the eigenvalues of $\mathscr{L}^{[l]}$ be the diagonal matrix $\Lambda^{[l]} = \text{diag}\{0 = \gamma_1^{[l]}, \gamma_2^{[l]}, \ldots, \gamma_N^{[l]}\}$ and $V^{[l]}$ be the orthogonal matrix, whose columns are the orthogonal eigenvectors of $\mathscr{L}^{[l]} (l = 1, 2)$.

Following the procedure proposed by *Watts* and *Strogatz* (WS)[16], the small-world networks are formed. For that we begin by considering a regular ring network of N nodes, each of which is connected to its $2k$ nearest neighbors (k on each side). Then we reconnect all the initial edges to the vertices chosen uniformly at random from distant nodes with probability p, where dual edges are not to be taken. Hence $2k$ be the average degree of intralayer electrical synaptic networks. Here we consider the complete multiplex network. For incomplete multiplex network (i.e., few replicas are connected and few are not) intralayer synchronization manifold will not be an invariant manifold, so it doesn't yield complete intralayer synchronization. Hence for the intralayer synchronization to exist, complete multiplex network is necessary.

Since the intralayer coupling function is of diffusive nature and the nonlinear interlayer coupling function is associated with each replica, and if all oscillators in each individual layers start with the same initial condition, then the velocity profiles

of all subsystems in each individual layer become the same. This ensures that the complete intralayer synchronization state $(\mathbf{x}_i, \mathbf{y}_i) = (\mathbf{x}_0, \mathbf{y}_0),\ i = 1, 2, \ldots, N$ is an invariant state for all coupling strengths ϵ and g_c. We call the subset

$$\mathcal{S} = \{(\mathbf{x}_0, \mathbf{y}_0) \subset \mathbb{R}^d : (\mathbf{x}_i, \mathbf{y}_i) = (\mathbf{x}_0, \mathbf{y}_0),\ i = 1, 2, \ldots, N\} \tag{2}$$

as synchronization manifold. The local stability of $\mathcal{S}$ can be determined by the intra- and interlayer coupling strengths and the spectral properties of the intralayer Laplacian matrices.

3 Numerical results

Now the two intralayer networks corresponding to the electrical synapses are statistically equivalent to each other due to the choice of identical WS network parameters k, and p_{sw} for both the layers. In this section, our main aim was to explore the effect of network parameters k, p_{sw}, inter- and intralayer coupling strengths g_c and ϵ on the emergence of intralayer synchronization state. We integrate equation (1) using fifth order Runge–Kutta–Felhberg method with integration time step $dt = 0.01$ and random initial conditions from the phase space volume $[-2.5, 2.0] \times [0, 30] \times [-4.3, -1.2]$. To draw the following parameter regions, we have taken 20 network realizations at each point. For a multiplex network merely two distinctive forms of synchronization states can emerge, namely, intralayer and interlayer synchronizations. Interlayer synchronization occurs when each unit in a given layer evolves synchronously with its replicas, regardless of whether or not it is synchronized with the other units of the same layer. Contrariwise, intralayer synchronization is defined as the state of synchrony in each of the individual layer, irrespective of the synchrony between the replica nodes. If each layer evolves synchronously then the synchronization error for layer-l $(l = 1, 2)$ is defined as

$$E_l = \lim_{T\to\infty} \frac{1}{T} \int_0^T \sum_{j=2}^{N} \frac{\sqrt{(x_{l1} - x_{lj})^2 + (y_{l1} - y_{lj})^2 + (z_{l1} - z_{lj})^2}}{N-1}\, dt, \tag{3}$$

where T is the long-time interval. Then the intralayer synchronization error of the multiplex network is defined as

$$E = \frac{E_1 + E_2}{2}. \tag{4}$$

To calculate the intralayer synchronization error, we simulate the entire dynamical network for 3×10^5 time steps with an integration time step of 0.01, and the transient is considered up to time steps 2×10^5.

In the presence of both the synaptic couplings, the neuronal multiplex network achieves intralayer synchronization with different firing patterns, results are shown in Figure 1 with fixed average degree $k = 2$ and small-world probability $p_{sw} = 0.15$. Each layer oscillates in complete synchronous motion with chaotic square wave bursting for the lower values of synaptic strengths $\epsilon = 8.0$ and $g_c = 0.3$. The chaotic square wave bursting time series are shown in Figure 1a, the corresponding attractors are shown in (x, y, z) plane in Figure 1b. The dynamics of layer-1 and layer-2 are represented by blue and red lines respectively. These figures show that both the layers are in synchronized square-wave bursting state, although their synchronization manifolds are different. Here the intralayer synchronization occurs. Increasing the values of the two coupling strengths to $\epsilon = 12.0$ and $g_c = 1.2$, each layer exhibits triangular firing

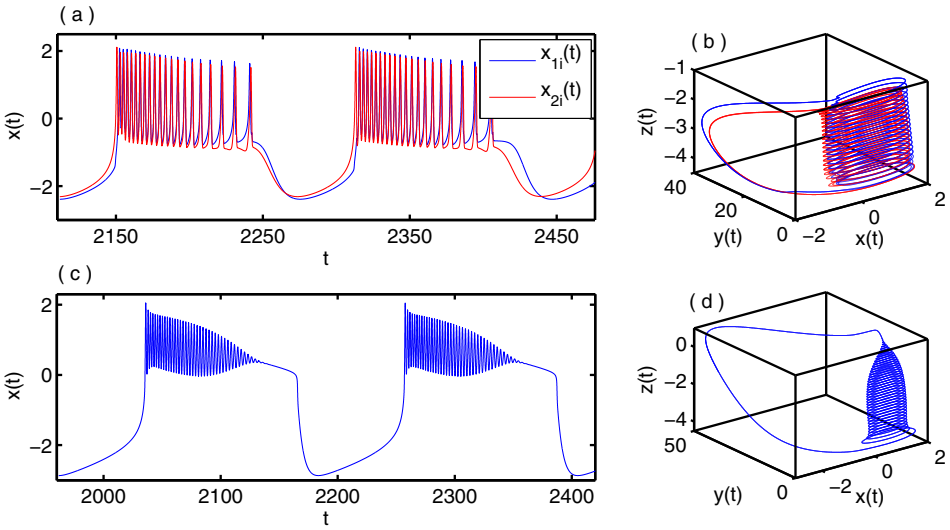

Fig. 1. (a,b) Intralayer synchronization and (c,d) global synchrony in the multiplex network. The first column represents the time series where each layer is in complete synchronization state various synaptic coupling strengths, while second column show the phase space of the synchronized manifolds. The first row (a,b) and second row (c,d) are plotted for $\epsilon = 8.0,\ g_c = 0.3$ and $\epsilon = 12.0,\ g_c = 1.2$ respectively. Other parameters are fixed at $k = 2$ and $p_{sw} = 0.15$.

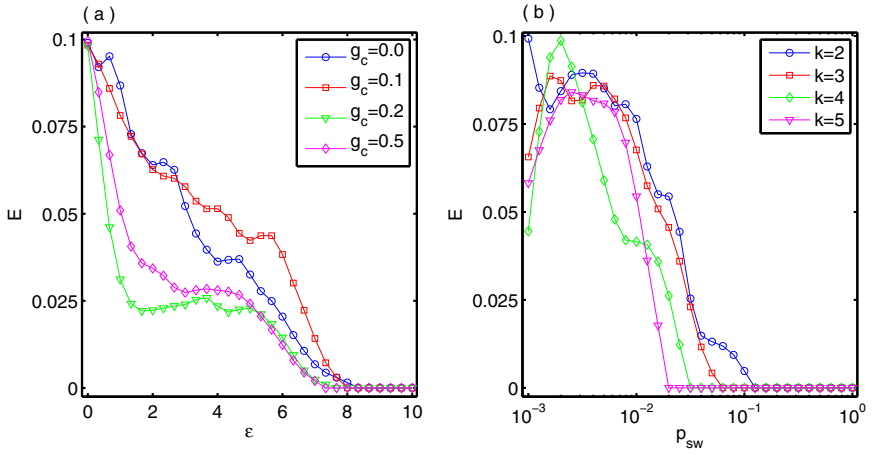

Fig. 2. Variation of the synchronization error by varying (a) ϵ for different values of g_c, where $p_{sw} = 0.15$ and $k = 2$; (b) p_{sw} for various values of k, with $\epsilon = 8.0$ and $g_c = 0.5$.

pattern in Figure 1c, and the corresponding plateau bursting state is manifested by the attractor in Figure 1d. Interestingly, we get the intralayer synchronization state where each replica is also completely synchronized. Here each replica also achieves the complete synchrony, hence the phase space. Figure 1d delineates global synchronization manifold. The higher coupling strength promotes two synchronized layers to evolve in unison. The blue trajectory in Figure 1d stands for the global synchronization manifold (simultaneous existence of intra- and interlayer synchrony) of the entire multiplex network.

Next we investigate the role of synaptic interaction strengths and the network parameters (g_c, p_{sw}) to emerge this intralayer synchronization state in the multiplex neuronal network. The results are presented in Figure 2. Figure 2a shows the average synchronization error with respect to the intralayer coupling strength ϵ by taking several exemplifying values of the chemical synaptic interaction strength g_c. Blue, red, green and magenta curves recount respective values of $g_c = 0.0,\ 0.1,\ 0.2$ and 0.5 for fixed $k = 2$ and $p_{sw} = 0.15$. Here slide enhancement of the synchrony is observed with respect to the interlayer strength g_c. When both the layers are uncoupled, then complete synchrony of these two layers occurs at $\epsilon = 8.33$. In the presence of interlayer interaction strength $g_c = 0.1$, the critical threshold value for intralayer synchrony occurs at $\epsilon = 8.0$. With a further increase in the interlayer chemical synaptic strength at $g_c = 0.2$, intralayer synchrony is observed for $\epsilon \geq 7.667$. In this way with increasing value of $g_c = 0.5$, the critical value of intralayer coupling strength $\epsilon \geq 7.33$ decreases. Recently similar results are observed in multilayer network [69,70].

Now we investigate the effect of small-world probability p_{sw} by changing the average degree k. The variations of the synchronization errors with respect to p_{sw} are shown in Figure 2b for various values of the average degree k of the small-world network (blue: $k = 2$, red: $k = 3$, green: $k = 4$, magenta: $k = 5$). Here we observe a significant enhancement of the intralayer synchronization with respect to k. For lower average degree $k = 2$, the synchrony occurs at $p_{sw} = 0.1259$. When we increase the average degree by setting $k = 3$, the synchronization appears at $p_{sw} = 0.0631$ which is much lower than that of the critical threshold for $k = 2$ case. The tendency of such an enhancement of intralayer synchrony is still preserved for more higher values of the average degree. For illustrated values of $k = 4$ and $k = 5$, the synchrony occurs for more lower values at $p_{sw} = 0.03162$ and $p_{sw} = 0.02$ respectively. So, from this scenario one can conclude, with a fixed character of network property (as fixed values of k and p_{sw}), interlayer interaction strength has not much of a significant effect on the intralayer synchronization property, while the variation of the network properties has a great impact on the enhancement of intralayer neural synchrony for fixed synaptic strengths.

4 Linear stability analysis

Using master stability function (MSF) approach in this section, we analyze the stability of the intralayer synchronization state in the multiplex network given by equation (1). We rewrite equation (1) as

$$\begin{aligned}
\dot{x}_{1i} &= f(x_{1i}, y_{1i}, z_{1i}) - \epsilon \sum_{j=1}^{N} \mathscr{L}_{ij}^{[1]} x_{1j} + g_c(v_s - x_{1i})\ \Gamma(x_{2i}),\\
\dot{y}_{1i} &= g(x_{1i}, y_{1i}, z_{1i}),\\
\dot{z}_{1i} &= h(x_{1i}, y_{1i}, z_{1i}),\\
\dot{x}_{2i} &= f(x_{2i}, y_{2i}, z_{2i}) - \epsilon \sum_{j=1}^{N} \mathscr{L}_{ij}^{[2]} x_{2j} + g_c(v_s - x_{2i})\ \Gamma(x_{1i}),\\
\dot{y}_{2i} &= g(x_{2i}, y_{2i}, z_{2i}),\\
\dot{z}_{2i} &= h(x_{2i}, y_{2i}, z_{2i}),
\end{aligned} \tag{5}$$

for $i = 1, 2, \ldots, N$, where $f(x, y, z) = (a - x)x^2 - y - z,\ g(x, y, z) = (a + \alpha)x^2 - y,\ h(x, y, z) = \mu(bx + c - z)$. Here each oscillator is identical and coupled by bidirectional small-world electrical network. The individual dynamics and the coupling term are all continuously differentiable. So through the MSF approach, we obtain the necessary and sufficient condition for the existence of the synchronized state.

When the intralayer synchronization occurs, let layer-1 evolves synchronously with synchronization state variable $\big(x_1(t), y_1(t), z_1(t)\big)$ and layer-2 with $\big(x_2(t), y_2(t), z_2(t)\big)$. This synchronization manifold satisfies the evolution equation

$$\begin{aligned}
\dot{x}_1 &= f(x_1, y_1, z_1) + g_c(v_s - x_1)\ \Gamma(x_2),\\
\dot{y}_1 &= g(x_1, y_1, z_1),\\
\dot{z}_1 &= h(x_1, y_1, z_1),\\
\dot{x}_2 &= f(x_2, y_2, z_2) + g_c(v_s - x_2)\ \Gamma(x_1),\\
\dot{y}_2 &= g(x_2, y_2, z_2),\\
\dot{z}_2 &= h(x_2, y_2, z_2).
\end{aligned} \tag{6}$$

Consider the small perturbations of the ith node in each layer from its synchronization manifold, its present state variable becomes $\big(x_{1i}, y_{1i}, z_{1i}\big) = \big(x_1 + \delta x_{1i}, y_1 + \delta y_{1i}, z_1 + \delta z_{1i}\big)$ and $\big(x_{2i}, y_{2i}, z_{2i}\big) = \big(x_2 + \delta x_{2i}, y_2 + \delta y_{2i}, z_2 + \delta z_{2i}\big)$. For the small perturbations and expanding around the intralayer synchronous manifold up to first order, we obtain the linearized equations of the error systems as

$$\begin{aligned}
\delta\dot{x}_{1i} &= f_x(x_1, y_1, z_1)\delta x_{1i} + f_y(x_1, y_1, z_1)\delta y_{1i} + f_z(x_1, y_1, z_1)\delta z_{1i}\\
&\quad - \epsilon \sum_{j=1}^{N} \mathscr{L}_{ij}^{[1]} \delta x_{1j} - g_c\Gamma(x_2)\delta x_{1i} + g_c(v_s - x_1)\ \Gamma_x(x_2)\delta x_{2i},\\
\delta\dot{y}_{1i} &= g_x(x_1, y_1, z_1)\delta x_{1i} + g_y(x_1, y_1, z_1)\delta y_{1i} + g_z(x_1, y_1, z_1)\delta z_{1i},\\
\delta\dot{z}_{1i} &= h_x(x_1, y_1, z_1)\delta x_{1i} + h_y(x_1, y_1, z_1)\delta y_{1i} + h_z(x_1, y_1, z_1)\delta z_{1i},\\
\delta\dot{x}_{2i} &= f_x(x_2, y_2, z_2)\delta x_{2i} + f_y(x_2, y_2, z_2)\delta y_{2i} + f_z(x_2, y_2, z_2)\delta z_{2i}\\
&\quad - \epsilon \sum_{j=1}^{N} \mathscr{L}_{ij}^{[2]} \delta x_{2j} - g_c\Gamma(x_1)\delta x_{2i} + g_c(v_s - x_2)\ \Gamma_x(x_1)\delta x_{1i},\\
\delta\dot{y}_{2i} &= g_x(x_2, y_2, z_2)\delta x_{2i} + g_y(x_2, y_2, z_2)\delta y_{2i} + g_z(x_2, y_2, z_2)\delta z_{2i},\\
\delta\dot{z}_{2i} &= h_x(x_2, y_2, z_2)\delta x_{2i} + h_y(x_2, y_2, z_2)\delta y_{2i} + h_z(x_2, y_2, z_2)\delta z_{2i},
\end{aligned} \tag{7}$$

where $i = 1, 2, \ldots, N$ and $f_x,\ f_y$ and f_z respectively denote the partial derivative of f with respect to x, y and z.

The above system has $6N$ Lyapunov exponents, among them six are parallel to the intralayer synchronization manifold, remaining $6N - 6$ are in the transverse direction to the synchronization manifold. The intralayer synchronization manifold will be stable if all the transverse Lyapunov exponents are negative. So among $6N$ Lyapunov exponents, we have to separate out the parallel and transverse components. For that, we spectrally decompose the perturbation vectors $\big(\delta x_{1i}, \delta y_{1i}, \delta z_{1i}\big)$ and $\big(\delta x_{2i}, \delta y_{2i}, \delta z_{2i}\big)$ onto the eigenspace of the Laplacian matrix corresponding to one of the layers. To enact this projection the choice of the layer is completely arbitrary. Since the eigenvectors of the Laplacian matrices for each layer form two equivalent bases of $\mathbb{R}^N$, we have chosen the eigenspace of $\mathscr{L}^{[1]}$, whose orthonormal eigenvectors form matrix $V^{[1]}$. Then the vector coefficient of the eigen decomposition of the error vectors of the two layers metamorphoses to

$$\Big(\xi_{1i}^{(x)}, \xi_{1i}^{(y)}, \xi_{1i}^{(z)}\Big) = \Big(\sum_{j=1}^{N} V_{ij}^{[1]}\delta x_{1j}, \sum_{j=1}^{N} V_{ij}^{[1]}\delta y_{1j}, \sum_{j=1}^{N} V_{ij}^{[1]}\delta z_{1j}\Big)$$

and $\Big(\xi_{2i}^{(x)}, \xi_{2i}^{(y)}, \xi_{2i}^{(z)}\Big) = \Big(\sum_{j=1}^{N} V_{ij}^{[1]}\delta x_{2j}, \sum_{j=1}^{N} V_{ij}^{[1]}\delta y_{2j}, \sum_{j=1}^{N} V_{ij}^{[1]}\delta z_{2j}\Big)$ respectively.

Therefore the dynamics of $\xi_{1i}^{(x)}$ for layer-1 is

$$\begin{aligned}\dot{\xi}_{1i}^{(x)} &= f_x(x_1,y_1,z_1)\xi_{1i}^{(x)} + f_y(x_1,y_1,z_1)\xi_{1i}^{(y)} \\ &\quad + f_z(x_1,y_1,z_1)\xi_{1i}^{(z)} - \epsilon\sum_{j=1}^{N} V_{ij}^{[1]}\sum_{k=1}^{N}\mathscr{L}_{jk}^{[1]}\delta x_{lk} \\ &\quad - g_c\Gamma(x_2)\xi_{1i}^{(x)} + g_c(v_s - x_1)\ \Gamma_x(x_2)\xi_{2i}^{(x)}. \end{aligned} \tag{8}$$

Here let $\left[V_{ij}^{[1]}\right]_{j=1}^{N}$ be the eigenvectors of $\mathscr{L}^{[1]}$ corresponding to eigenvalue $\gamma_i^{[1]}$, therefore

$$\sum_{j=1}^{N} V_{ij}^{[1]}\sum_{k=1}^{N}\mathscr{L}_{jk}^{[1]}\delta x_{1k} = \sum_{k=1}^{N}\gamma_i^{[1]}V_{ik}^{[1]}\delta x_{1k} = \gamma_i^{[1]}\xi_{1i}^{(x)}.$$

Putting the above expression in equation (8), it becomes

$$\begin{aligned}\dot{\xi}_{1i}^{(x)} &= f_x(x_1,y_1,z_1)\xi_{1i}^{(x)} + f_y(x_1,y_1,z_1)\xi_{1i}^{(y)} + f_z(x_1,y_1,z_1)\xi_{1i}^{(z)} - \epsilon\gamma_i^{[1]}\xi_{1i}^{(x)} \\ &\quad - g_c\Gamma(x_2)\xi_{1i}^{(x)} + g_c(v_s - x_1)\ \Gamma_x(x_2)\xi_{2i}^{(x)}. \end{aligned} \tag{9}$$

The dynamics of $\xi_{2i}^{(x)}$ for layer-2 is

$$\begin{aligned}\dot{\xi}_{2i}^{(x)} &= f_x(x_2,y_2,z_2)\xi_{2i}^{(x)} + f_y(x_2,y_2,z_2)\xi_{2i}^{(y)} + f_z(x_2,y_2,z_2)\xi_{2i}^{(z)} \\ &\quad - \epsilon\sum_{j=1}^{N} V_{ij}^{[1]}\sum_{k=1}^{N}\mathscr{L}_{jk}^{[2]}\delta x_{2k} - g_c\Gamma(x_1)\xi_{2i}^{(x)} + g_c(v_s - x_2)\ \Gamma_x(x_1)\xi_{1i}^{(x)}. \end{aligned} \tag{10}$$

Now, let $V^{[2]}$ be the matrix of eigenvectors of the Laplacian matrix $\mathscr{L}^{[2]}$ for layer-2. Hence $\mathscr{L}_{ij}^{[2]} = \sum_{r=1}^{N} V_{rj}^{[2]}\gamma_r^{[2]}V_{rj}^{[2]}$. From $\xi_{2i}^{(x)} = \sum_{j=1}^{N} V_{ij}^{[1]}\delta x_{2j}$, we get $\delta x_{2i} = \sum_{k=1}^{N} V_{ki}^{[1]}\xi_{2k}^{(x)}$. Thus, we have,

$$\sum_{j=1}^{N} V_{ij}^{[1]}\sum_{k=1}^{N}\mathscr{L}_{jk}^{[2]}\delta x_{2k} = \sum_{r=1}^{N}\sum_{l=1}^{N}\Big[\sum_{j=1}^{N} V_{ij}^{[1]}V_{rj}^{[2]}\Big]\gamma_r^{[2]}\Big[\sum_{k=1}^{N} V_{rk}^{[2]}V_{lk}^{[1]}\Big]\xi_{2l}^{(x)}. \tag{11}$$

Therefore equation (10) becomes

$$\begin{aligned}\dot{\xi}_{2i}^{(x)} &= f_x(x_2,y_2,z_2)\xi_{2i}^{(x)} + f_y(x_2,y_2,z_2)\xi_{2i}^{(y)} + f_z(x_2,y_2,z_2)\xi_{2i}^{(z)} \\ &\quad - \epsilon\sum_{r=1}^{N}\sum_{l=1}^{N}\Big[\sum_{j=1}^{N} V_{ij}^{[1]}V_{rj}^{[2]}\Big]\gamma_r^{[2]}\Big[\sum_{k=1}^{N} V_{rk}^{[2]}V_{lk}^{[1]}\Big]\xi_{2l}^{(x)} \\ &\quad - g_c\Gamma(x_1)\xi_{2i}^{(x)} + g_c(v_s - x_2)\ \Gamma_x(x_1)\xi_{1i}^{(x)}. \end{aligned}$$

For $i = 1$, $\gamma_i^{[1]} = 0$ and $r = 1$, $\gamma_r^{[2]} = 0$, hence the transformed equation reduces to the linearized equation of the synchronization manifold (Eq. (6)). So it evolves parallel to the synchronization dynamics. For $i \geq 2$, the linearized equation evolves transverse to the synchronization manifold.

For $l = 1$, let $\left[V_{lk}^{[1]}\right]_{k=1}^{N}$ be the eigenvector corresponding to eigenvalue 0. Now the eigenvectors are orthogonal to each other, so it is orthogonal to all other Laplacian

eigenvectors. Hence $\sum_{k=1}^{N} V_{rk}^{[2]} V_{lk}^{[1]}$ is equal to 1 if $r = 1$ and 0 otherwise ($l = 1, 2$). So, $\sum_{j=1}^{N}\sum_{k=1}^{N} V_{ij}^{[1]} \mathscr{L}_{jk}^{[2]} \delta x_{2k} = \sum_{r=2}^{N}\sum_{l=2}^{N} \Big[\sum_{j=1}^{N} V_{ij}^{[1]} V_{rj}^{[2]}\Big] \gamma_r^{[2]} \Big[\sum_{k=1}^{N} V_{rk}^{[2]} V_{lk}^{[1]}\Big] \xi_{2l}^{(x)}$.
Therefore according to this isomorphic transformation, the corresponding error dynamics (7) transformed as

$$
\begin{aligned}
\dot{\xi}_{1i}^{(x)} &= f_x(x_1, y_1, z_1)\xi_{1i}^{(x)} + f_y(x_1, y_1, z_1)\xi_{1i}^{(y)} + f_z(x_1, y_1, z_1)\xi_{1i}^{(z)} - \epsilon\gamma_i^{[1]}\xi_{1i}^{(x)} \\
&\quad - g_c\Gamma(x_2)\xi_{1i}^{(x)} + g_c(v_s - x_1)\ \Gamma_x(x_2)\xi_{2i}^{(x)}, \\
\dot{\xi}_{1i}^{(y)} &= g_x(x_1, y_1, z_1)\xi_{1i}^{(x)} + g_y(x_1, y_1, z_1)\xi_{1i}^{(y)} + g_z(x_1, y_1, z_1)\xi_{1i}^{(z)}, \\
\dot{\xi}_{1i}^{(z)} &= h_x(x_1, y_1, z_1)\xi_{1i}^{(x)} + h_y(x_1, y_1, z_1)\xi_{1i}^{(y)} + h_z(x_1, y_1, z_1)\xi_{1i}^{(z)}, \\
\dot{\xi}_{2i}^{(x)} &= f_x(x_2, y_2, z_2)\xi_{2i}^{(x)} + f_y(x_2, y_2, z_2)\xi_{2i}^{(y)} + f_z(x_2, y_2, z_2)\xi_{2i}^{(z)} \\
&\quad - \epsilon\sum_{r=2}^{N}\sum_{l=2}^{N}\Big[\sum_{j=1}^{N} V_{ij}^{[1]} V_{rj}^{[2]}\Big]\gamma_r^{[2]}\Big[\sum_{k=1}^{N} V_{rk}^{[2]} V_{lk}^{[1]}\Big]\xi_{2l}^{(x)} - g_c\Gamma(x_1)\xi_{2i}^{(x)} \\
&\quad + g_c(v_s - x_2)\ \Gamma_x(x_1)\xi_{1i}^{(x)}, \\
\dot{\xi}_{2i}^{(y)} &= g_x(x_2, y_2, z_2)\xi_{2i}^{(x)} + g_y(x_2, y_2, z_2)\xi_{2i}^{(y)} + g_z(x_2, y_2, z_2)\xi_{2i}^{(z)}, \\
\dot{\xi}_{2i}^{(z)} &= h_x(x_2, y_2, z_2)\xi_{2i}^{(x)} + h_y(x_2, y_2, z_2)\xi_{2i}^{(y)} + h_z(x_2, y_2, z_2)\xi_{2i}^{(z)}.
\end{aligned} \tag{12}
$$

where $i = 1, 2, \ldots, N$. For our case, the two small-world networks in the two layers are topologically equivalent, since for both the layers, the network parameters are taken identical, though the two networks may not be identical because of random rewiring of the edges. In that case, the two Laplacian matrices may not be commutative.

The eigenvector corresponding to the zero eigenvalue yields the parallel direction, and other eigenvectors for transverse directions. The partial derivatives are appraised as $f_x(x, y, z) = (2a - 3x)x$, $f_y(x, y, z) = -1$, $f_z(x, y, z) = -1$; $g_x(x, y, z) = 2(a + \alpha)x$, $g_y(x, y, z) = -1$, $g_z(x, y, z) = 0$; $h_x(x, y, z) = \mu b$, $h_y(x, y, z) = 0$, $h_z(x, y, z) = -\mu$ and $\Gamma_x(x) = \frac{\lambda \exp[-\lambda(x-\Theta_s)]}{\left[1+\exp[-\lambda(x-\Theta_s)]\right]^2}$. Putting this partial derivatives into equation (12), our required transverse error systems become

$$
\begin{aligned}
\dot{\xi}_{1i}^{(x)} &= (2a - 3x_1)x_1\xi_{1i}^{(x)} - \xi_{1i}^{(y)} - \xi_{1i}^{(z)} - \epsilon\gamma_i^{[1]}\xi_{1i}^{(x)} - \tfrac{g_c}{1+\exp[-\lambda(x_2-\Theta_s)]}\xi_{1i}^{(x)} \\
&\quad + g_c(v_s - x_1)\ \tfrac{\lambda \exp[-\lambda(x_2-\Theta_s)]}{\left[1+\exp[-\lambda(x_2-\Theta_s)]\right]^2}\xi_{2i}^{(x)}, \\
\dot{\xi}_{1i}^{(y)} &= 2(a + \alpha)x_1\xi_{1i}^{(x)} - \xi_{1i}^{(y)}, \\
\dot{\xi}_{1i}^{(z)} &= \mu\Big(b\xi_{1i}^{(x)} - \xi_{1i}^{(z)}\Big), \\
\dot{\xi}_{2i}^{(x)} &= (2a - 3x_2)x_2\xi_{2i}^{(x)} - \xi_{2i}^{(y)} - \xi_{2i}^{(z)} - \epsilon\sum_{r=2}^{N}\sum_{l=2}^{N}\Big[\sum_{j=1}^{N} V_{ij}^{[1]} V_{rj}^{[2]}\Big]\gamma_r^{[2]}\Big[\sum_{k=1}^{N} V_{rk}^{[2]} V_{lk}^{[1]}\Big]\xi_{2l}^{(x)} \\
&\quad - \tfrac{g_c}{1+\exp[-\lambda(x_1-\Theta_s)]}\xi_{2i}^{(x)} + g_c(v_s - x_2)\ \tfrac{\lambda \exp[-\lambda(x_1-\Theta_s)]}{\left[1+\exp[-\lambda(x_1-\Theta_s)]\right]^2}\xi_{1i}^{(x)}, \\
\dot{\xi}_{2i}^{(y)} &= 2(a + \alpha)x_2\xi_{2i}^{(x)} - \xi_{2i}^{(y)}, \\
\dot{\xi}_{2i}^{(z)} &= \mu\Big(b\xi_{2i}^{(x)} - \xi_{2i}^{(z)}\Big), \quad i = 2, 3, \ldots, N.
\end{aligned} \tag{13}
$$

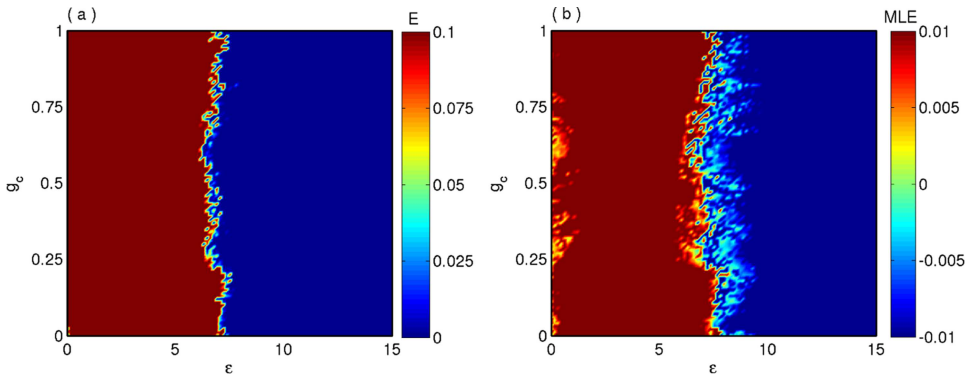

Fig. 3. Variation of (a) the synchronization error and (b) the maximum transverse Lyapunov exponent in the parameter space of the interaction strengths ϵ and g_c with fixed values of $k = 2$ and $p_{sw} = 0.15$.

The synchronization state variables (x_1, y_1, z_1) and (x_2, y_2, z_2) obey the equations of motion,

$$\begin{aligned}
\dot{x}_1 &= (a - x_1)x_1^2 - y_1 - z_1 + g_c(v_s - x_1)\ \Gamma(x_2),\\
\dot{y}_1 &= (a + \alpha)x_1^2 - y_1,\\
\dot{z}_1 &= \mu(bx_1 + c - z_1),\\
\dot{x}_2 &= (a - x_2)x_2^2 - y_2 - z_2 + g_c(v_s - x_2)\ \Gamma(x_1),\\
\dot{y}_2 &= (a + \alpha)x_2^2 - y_2,\\
\dot{z}_2 &= \mu(bx_2 + c - z_2).
\end{aligned} \tag{14}$$

To reveal the complete transition scenarios of intralayer neuronal synchrony in the multiplex network, we draw the synchrony and desynchrony regions in the (ϵ, g_c) plane in Figure 3 for the fixed values of $k = 2$ and $p_{sw} = 0.15$. Here the neuronal synchrony is measured by quantity E and the existence is characterized through the master stability function approach. In the color coded Figure 3a, the deep blue and red regions correspond to synchronization and desynchronization states respectively, whereas the color bar denotes the variation of the intralayer synchronization error E. The transition from desynchrony to synchrony is almost vertical in the (ϵ, g_c) plane but in a very narrow region in this space there is a roughened type of transition (i.e., synchrony to desynchrony to synchrony). The stability of such a transition is characterized by the MSF theory and the corresponding result is drawn in Figure 3b. The color bar of Figure 3b represents the variation of the maximum Lyapunov exponent (MLE). Negative values of the MLE signify the appearance of the synchronized motions. Here in the deep blue region, the color bar takes negative values which indicates the occurrence of the intralayer neuronal synchrony and it verifies the transition scenarios of Figure 3a.

Next we investigate the simultaneous effect of small world probability p_{sw} and intralayer coupling strength ϵ on the transition scenarios of intralayer neuronal synchrony in the entire multiplex network for fixed interlayer interaction $g_c = 0.3$ and network average degree $k = 2$. The transition scenarios are delineated in Figure 4 in the (ϵ, p_{sw}) plane. By calculating the intralayer synchronization error E, the transition from desynchrony to synchrony states are described in Figure 4a where the color bar shows the variation of E. The deep red and blue areas represent the desynchronization and synchronization states respectively. Here it is observed that the

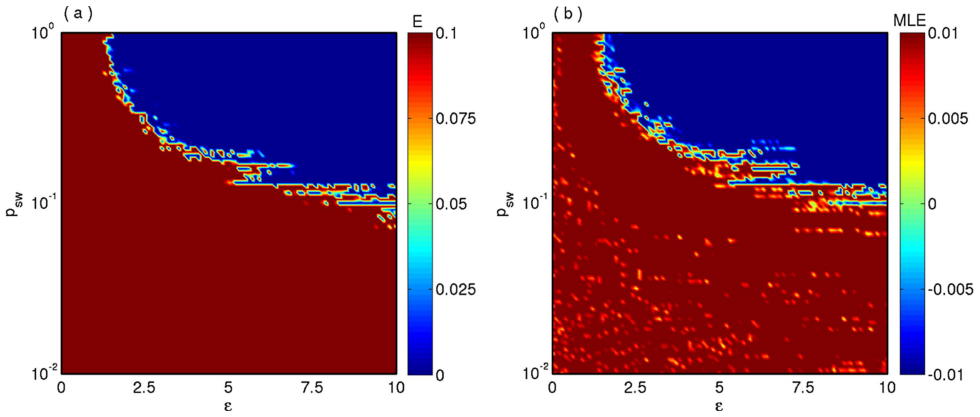

Fig. 4. (a) Synchronization error and (b) transverse maximum Lyapunov exponents in (ϵ, p_{sw}) parameter space, for $g_c = 0.3$ and $k = 2$.

critical transition point of intralayer coupling values for the synchrony is monotonically decreasing with the increased values of the small-world probability p_{sw}. The stability of such transitions is characterized by the MSF framework in Figure 4b. The color bar of Figure 4b denotes the variation of MSF and this figure clearly verifies the transition scenarios as in Figure 4a. So, from the results as in Figures 3 and 4, one can conclude that the combined effect of the intra and interlayer coupling strengths has not much of a significant effect on the enhancement of intralayer neuronal synchrony in the multiplex neuronal network whereas the combined effect of the intralayer coupling strength and the small world probability induced significant changes on the enhancement of the intralayer neuronal synchrony in the entire multiplex neuronal network.

5 Conclusion

In this paper, we have investigated neuronal synchrony in the multiplex neuronal network. Mainly, we explored the intralayer neuronal synchronization under the simultaneous effect of the synaptic interactions. In our study, we have considered that each layer is associated with the small-world architecture. The intention behind the consideration of such a network formation is the *small-world* characteristic of the brain network [67,68]. As enormous amounts of neurons are involved in the inter neuronal communications, neurons normally perform in the lumped or highly clotted basis. In that case multilayer or modular organization is the best representation of the neuronal network. Each node of the multiplex network is cast by the Hindmarsh–Rose neuronal oscillator. Here we have considered that the interaction among the neurons within each layer happens through the electric synapses by making a gap junction between the adjacent neurons while the interlayer connections are taken as chemical synaptic interactions. It is observed that the combined effect of both types of synaptic couplings does not have any indicative change on the enhancement of intralayer neuronal synchrony property whereas the simultaneous effect of small-world probability and intralayer coupling plays a crucial role on the enhancement of intralayer neuronal synchrony in the multiplex neuronal network. Through the master stability approach, we analytically derived the necessary condition for intralayer neuronal synchrony and the analytical findings are confirmed by numerical results.

D.G. was supported by SERB-DST (Department of Science and Technology), Government of India (Project no. EMR/2016/001039).

References

1. S. Boccaletti, V. Latora, Y. Moreno, M. Chavez, D.-U. Hwang, Phys. Rep. **424**, 175 (2006)
2. S.H. Strogatz, Nature **410**, 268 (2001)
3. R. Albert, A.-L. Barabási, Rev. Mod. Phys. **74**, 47 (2002)
4. M.E.J. Newman, SIAM Rev. **45**, 167 (2003)
5. A. Barrat, M. Barthélemy, A. Vespignani, *Dynamical Processes on Complex Networks*, (Cambridge Univ. Press, 2008)
6. B. Barzel, A.-L. Barabási, Nat. Phys. **9**, 673 (2013)
7. R. Banerjee, D. Ghosh, E. Padmanaban, R. Ramaswamy, L.M. Pecora, S.K. Dana, Phys. Rev. E **85**, 027201 (2012)
8. S. Boccaletti, *The Synchronized Dynamics of Complex Systems* (Elsevier, Amsterdam, 2008), Vol. 6
9. S. Majhi, D. Ghosh, Chaos **27**, 053115 (2017)
10. A. Arenas, A. Diaz-Guilera, J. Kurths, Y. Moreno, C. Zhou, Phys. Rep. **469**, 93 (2008)
11. D. Ghosh, S. Banerjee, Phys. Rev. E **78**, 056211 (2008)
12. D. Ghosh, P. Saha, A. Roy Chowdhury, Commun. Nonlinear Sci. Numer. Simul. **15**, 1640 (2010)
13. A. Pikovsky, J. Kurths, M. Rosenblum, *Synchronization: A Universal Concept in Nonlinear Sciences* (Cambridge University Press, Cambridge, 2013)
14. P. Erdös, A. Rényi, Publ. Math. Debrecen **6**, 290 (1959)
15. R. Albert, A.-L. Barabási, Science **286**, 590 (1999)
16. D.J. Watts, S.H. Strogatz, Nature **393**, 440 (1998)
17. F. Sorrentino, New J. Phys. **14**, 033035 (2012)
18. S. Rakshit, B.K. Bera, D. Ghosh, Phys. Rev. E **98**, 032305 (2018)
19. S. Rakshit, B.K. Bera, D. Ghosh, S. Sinha, Phys. Rev. E **97**, 052304 (2018)
20. B.L.M. Happel, J.M.J. Murre, Neural Netw. **7**, 985 (1994)
21. S. Boccaletti, G. Bianconi, R. Criado, C.I. del Genio, J. Gómez-Gardeñes, M. Romance, I. Sendiña-Nadal, Z. Wang, M. Zanin, Phys. Rep. **544**, 1 (2014)
22. M. Kivelä, A. Arenas, M. Barthelemy, J.P. Gleeson, Y. Moreno, M.A. Porter, J. Complex Networks **2**, 203 (2014)
23. G. Bianconi, *Multilayer Networks: Structure and Function* (Oxford University Press, Oxford, 2018)
24. S. Pilosof, M.A. Porter, M. Pascual, S. Kéfi, Nat. Ecol. Evol. **1**, 0101 (2017)
25. O. Yagan, D. Qian, J. Zhang, D. Cochran, IEEE J. Sel. Areas Commun. **31**, 1038 (2013)
26. A.E. Pereda, Nat. Rev. **15**, 250 (2014)
27. M. Szell, R. Lambiotte, S. Thurner, Proc. Natl. Acad. Sci. USA **107**, 13636 (2010)
28. A. Cardillo, J. Gómez-Gardeñes, M. Zanin, M. Romance, D. Papo, F. del Pozo, S. Boccaletti, Sci. Rep. **3**, 1344 (2013)
29. A. Halu, S. Mukherjee, G. Bianconi, Phys. Rev. E **89**, 012806 (2014)
30. A. Cardillo, M. Zanin, J. Gómez-Gardeñes, M. Romance, A. García del Amo, S. Boccaletti, Eur. Phys. J. Special Topics **215**, 23 (2013)
31. R. Criado, M. Romance, M. Vela-Pérez, Int. J. Bifurc. Chaos **20**, 877 (2010)
32. R. Criado, B. Hernández-Bermejo, M. Romance, Int. J. Bifurc. Chaos **17**, 2289 (2007)
33. C. Granell, S. Gómez, A. Arenas, Phys. Rev. Lett. **111**, 128701 (2013)
34. B. Bentley, R. Branicky, C.L. Barnes, Y.L. Chew, E. Yemini, E.T. Bullmore, P.E. Vértes, W.R. Schafer, PLoS Comput. Biol. **12**, e1005283 (2016)
35. S.V. Buldyrev, R. Parshani, G. Paul, H.E. Stanley, S. Havlin, Nature **464**, 1025 (2010)
36. J. Gao, S. V. Buldyrev, H. E. Stanley, S. Havlin, Nat. Phys. **8**, 40 (2012)
37. G. Bianconi, S.N. Dorogovtsev, Phys. Rev. E **89**, 062814 (2014)
38. S. Gómez, A. Díaz-Guilera, J. Gómez-Gardeñes, C.J. Pérez-Vicente, Y. Moreno, A. Arenas, Phys. Rev. Lett. **110**, 028701 (2013)
39. A. Saumell-Mendiola, M. Serrano, M. Boguñá, Phys. Rev. E **86**, 026106 (2012)
40. C. Buono, L.G. Alvarez-Zuzek, P.A. Macri, L.A. Braunstein, PLoS One **9**, e92200 (2014)

41. J. Sanz, C.-Y. Xia, S. Meloni, Y. Moreno, Phys. Rev. X **4**, 041005 (2014)
42. Z. Wang, A. Szolnoki, M. Perc, J. Theor. Biol. **349**, 50 (2014)
43. G. Menichetti, L. Dall'Asta, G. Bianconi, Sci. Rep. **6**, 20706 (2016)
44. M.V. Goremyko, V.A. Maksimenko, V.V. Makarov, D. Ghosh, B. Bera, S.K. Dana, A.E. Hramov, Tech. Phys. Lett. **43**, 712 (2017)
45. V.A. Maksimenko, M.V. Goremyko, V.V. Makarov, A.E. Hramov, D. Ghosh, B.K. Bera, S.K. Dana, Bull. Russ. Acad. Sci.: Phys. **81**, 110 (2017)
46. L.V. Gambuzza, M. Frasca, J. Gómez-Gardeñes, Europhys. Lett. **110**, 20010 (2015)
47. S. Rakshit, S. Majhi, B. K. Bera, S. Sinha, D. Ghosh, Phys. Rev. E **96**, 062308 (2017)
48. S. Majhi, D. Ghosh, J. Kurths, Phys. Rev. E **99**, 012308 (2019)
49. R. Sevilla-Escoboza, I. Sendiña-Nadal, I. Leyva, R. Gutiérrez, J.M. Buldú, S. Boccaletti, Chaos **26**, 065304 (2016)
50. I. Leyva, R. Sevilla-Escoboza, I. Sendiña-Nadal, R. Gutiérrez, J.M. Buldú, S. Boccaletti, Sci. Rep. **7**, 45475 (2017)
51. X. Zhang, S. Boccaletti, S. Guan, Z. Liu, Phys. Rev. Lett. **114**, 038701 (2015)
52. S. Majhi, T. Kapitaniak, D. Ghosh, Chaos **29**, 013108 (2019)
53. V.A. Maksimenko, V.V. Makarov, B.K. Bera, D. Ghosh, S.K. Dana, M.V. Goremyko, N.S. Frolov, A.A. Koronovskii, A.E. Hramov, Phys. Rev. E **94**, 052205 (2016)
54. S. Majhi, M. Perc, D. Ghosh, Sci. Rep. **6**, 39033 (2016)
55. S. Majhi, B.K. Bera, D. Ghosh, M. Perc, Phys. Life Rev. **28**, 100 (2019)
56. S. Majhi, M. Perc, D. Ghosh, Chaos **27**, 073109 (2017)
57. S. Jalan, A. Singh, Europhys. Lett. **113**, 30002 (2016)
58. P.J. Uhlhaas, G. Pipa, B. Lima, L. Melloni, S. Neuenschwander, D. Nikolić, W. Singer, Front. Integr. Neurosci. **3**, 17 (2009)
59. B.K. Bera, D. Ghosh, M. Lakshmanan Phys. Rev. E **93**, 012205 (2016)
60. B.K. Bera, D. Ghosh, T. Banerjee, Phys. Rev. E **94**, 012215 (2016)
61. B.K. Bera, D. Ghosh, Phys. Rev. E **93**, 052223 (2016)
62. P.J. Uhlhaas, W. Singer, Neuron **52**, 155 (2006)
63. R. Llinas, U. Ribary, Proc. Natl. Acad. Sci. USA **90**, 2078 (1993)
64. W. Singer, C.M. Gray, Annu. Rev. Neurosci. **18**, 555 (1995)
65. D.K. Hartline, Biol. Cybern. **33**, 223 (1979)
66. R. Bartsch, J.W. Kantelhardt, T. Penzel, S. Havlin, Phys. Rev. Lett. **98**, 054102 (2007)
67. D.S. Bassett, E.D. Bullmore, Neuroscientist **12**, 512 (2006)
68. D.S. Bassett, E.D. Bullmore, Neuroscientist **23**, 499 (2017)
69. W.J. Yuan, J.F. Zhou, I.S. Nadal, S. Boccaletti, Z. Wang, Phys. Rev. E **97**, 022211 (2018)
70. I. Leyva, I.S. Nadal, R.S. Escoboza, V.P. Vera-Avila, P. Chholak, S. Boccaletti, Sci. Rep. **8**, 8629 (2018)